Environ Sci Pollut Res (2013) 20:227–237
DOI 10.1007/s11356-012-0971-4

RESEARCH ARTICLE

Seasonal and air mass trajectory effects on dissolved organic matter of bulk deposition at a coastal town in south-western Europe

Patrícia S. M. Santos · Eduarda B. H. Santos · Armando C. Duarte

Received: 17 January 2012 / Accepted: 7 May 2012 / Published online: 31 May 2012

Abstract Rainwater contains a complex mixture of organic compounds which may influence climate, terrestrial and maritime ecosystems and thus human health. In this work, the characteristics of DOM of bulk deposition at a coastal town on the southwest of Europe were assessed by UV–visible and three-dimensional excitation–emission matrix fluorescence spectroscopies and by dissolved organic carbon (DOC) content. The seasonal and air mass trajectory effects on dissolved organic matter (DOM) of bulk deposition were evaluated. The absorbance at 250 nm (UV_{250nm}) and integrated fluorescence showed to be positively correlated with each other, and they were also positively correlated to the DOC in bulk deposition, which suggest that a constant fraction of DOM is likely to fluoresce. There was more chromophoric dissolved organic matter (CDOM) present in summer and autumn seasons than in winter and spring. Bulk deposition associated with terrestrial air masses contained a higher CDOM content than bulk deposition related to marine air masses, thus highlighting the contribution of terrestrial/anthropogenic sources.

Keywords Rainwater · DOM · UV–visible spectroscopy · Fluorescence spectroscopy · Seasonal variation · Air mass trajectory

Responsible editor: Euripides Stephanou

P. S. M. Santos · E. B. H. Santos · A. C. Duarte (✉)
CESAM (Centre for Environmental and Marine Studies)
& Department of Chemistry, University of Aveiro,
Campus Universitário de Santiago,
3810-193 Aveiro, Portugal
e-mail: aduarte@ua.pt

Introduction

Dissolved organic matter (DOM), quantified as dissolved organic carbon (DOC), is a ubiquitous component of rainwater and is a major component of both marine (23 μM DOC) and continental rain (161 μM DOC) (Willey et al. 2000). DOM in rainwater is a complex mixture of organic compounds (Seitzinger et al. 2003), and rainwater is a globally important removal mechanism for atmospheric DOC, with a carbon flux (0.3 Gt $year^{-1}$) equal to approximately 6 % of the fossil fuel influx (5.5 Gt $year^{-1}$) to the atmosphere (Willey et al. 2000).

Recent studies (Kieber et al. 2006; Muller et al. 2008; Miller et al. 2009; Mladenov et al. 2009; Santos et al. 2009a,b) have demonstrated that chromophoric dissolved organic matter (CDOM) is an important constituent of rainwater. CDOM is also an important fraction of the water-soluble organic matter (WSOM) in atmospheric particles (Facchini et al. 1999; Zappoli et al. 1999; Decesari et al. 2000; Duarte et al. 2005) exhibiting intense absorbance in the lower visible to UV range and, therefore, they might also be important in atmospheric absorption of solar radiation (Hoffer et al. 2004). These organic constituents were found to be important contributors to cloud condensation nuclei (CCN) (Facchini et al. 1999; Gysel et al. 2004). Furthermore, droplet clouds are effective reflectors of incoming solar radiation, and small perturbations in their properties can significantly impact the amount of solar radiation absorbed by the planet, which consequently affect climate (Andreae et al. 2005). Thus, WSOM of atmospheric particles as well as DOM of rainwater may influence climate. Moreover, DOM in rainwater is also important since rain is the predominant source of all

fresh water and its composition may affect both terrestrial and aquatic ecosystems.

DOM in rainwater is still poorly characterised with respect to the chemical compounds present, their sources, temporal and spatial patterns of variation, and the subsequent impact on climate and the environment (Muller et al. 2008). To the best of our knowledge, only six recent studies have addressed the optical properties of the bulk CDOM of rainwater with the purpose of evaluating some of the abovementioned points (Kieber et al. 2006; Muller et al. 2008; Miller et al. 2009; Mladenov et al. 2009; Santos et al. 2009b; Cheng et al. 2010).

Kieber et al. (2006) determined the DOC content and analysed the UV–visible and excitation–emission matrix (EEM) fluorescence properties of rainwater in Wilmington (North Carolina, USA) to study the CDOM and its variation with air mass back trajectories and seasonality. Muller et al. (2008) also determined the EEM fluorescence properties of rainwater in Birmingham (UK) and analysed its variations with meteorological patterns (storm type, source area and air mass type). Miller et al. (2009) used UV absorbance and EEM fluorescence spectroscopy together with the DOC content to define the chemical characteristics of CDOM in whole rainwater. Mladenov et al. (2009) characterised CDOM in wet deposition using UV–visible absorbance and EEM fluorescence spectroscopy. Santos et al. (2009b) evaluated the variability of the optical properties of CDOM in bulk deposition of Aveiro (Portugal), for similar air mass trajectories (maritime), between autumn and winter events, using the DOC content, and the UV–visible and the EEM fluorescence spectroscopies. Cheng et al. (2010) analysed the optical characteristics of CDOM in rain collected in Xiamen Island (China), during the rainy season of 2007, using a combination of UV–visible and the EEM fluorescence spectroscopies.

The main aims of this work are to characterise the DOM present in bulk deposition at a coastal town (Aveiro, Portugal) in south-western Europe and to evaluate how that DOM was affected by seasons, type of air mass and source area using back-trajectory analysis. For such purposes, 40 bulk deposition samples were collected between September 2008 and September 2009, and were assessed using UV–visible and EEM fluorescence spectroscopies and DOC concentrations. The data set is unique because it was collected for a long period and represents one of the first detailed studies of bulk deposition DOM in Western Europe. Moreover, the results of this work will contribute to the broader knowledge of the general properties of rainwater and atmospheric DOM, and it will provide information regarding the general characteristics of DOM observed in rainwater from other locations (Kieber et al. 2006; Muller et al. 2008) and if they are generally relevant to south-western Europe.

Experimental

Bulk deposition sampling and sample preparation

Bulk deposition was collected at a sampling station (40°38′ N, 8°39′ W) located in the western part of the town of Aveiro, Portugal, between September 2008 and September 2009. The sample collection was carried out at 70 cm above the ground, through glass funnels (30 cm diameter) into glass bottles (5 L), placed inside PVC opaque tubes, being the samples protected from direct sunlight. The sampling containers were left open in order to collect the bulk deposition (both wet and dry depositions) on a 24-h basis. Compositional changes may have occurred upon storage in the sample collectors especially in the warm summer months. Prior to use, all glass materials were immersed for 30 min, in a solution of NaOH (0.1 M), then rinsed with distilled water, followed by another immersion for 24 h in a solution of HNO_3 (4 M), and finally rinsed with ultrapure (Milli-Q) water. After collection, samples were transported to the laboratory where they were filtered through hydrophilic PVDF Millipore membrane filters (0.45 μm). For all the sampling episodes, one aliquot of sample was stored in glass vials in the dark at 4 °C for a maximum of 4 days, for subsequent optical analysis, and another aliquot was frozen for subsequent analysis of DOC content. The storage of samples in the dark at 4 °C was proved to be adequate for keeping the optical properties of the samples unchanged as long as the storage time does not exceed 4 days (Santos et al. 2010).

Measurements of dissolved organic carbon (DOC)

The DOC concentration was measured for each sample using a Shimadzu TOC-5000A analyser. First, the concentrations of total carbon (TC) and inorganic carbon (IC) were measured and then the DOC concentration of samples was calculated as the difference (TC−IC). For TC quantification, standards were prepared from reagent grade potassium hydrogen phthalate in ultrapure water in the range of 0.5 to 2 mg CL^{-1}. For IC measurements, standards were performed from reagents grade sodium hydrogenocarbonate plus sodium carbonate in ultrapure water, also in the range of 0.5 to 2 mg CL^{-1}. Control standards were generally within 5 % agreement in terms of TC and IC content. For each sample, three replicates were analysed for determining the average DOC content.

Optical analysis

UV–visible spectra (in the range of 200–600 nm) of samples were recorded on a Shimadzu (Dusseldorf, Germany) Model UV 210PC spectrophotometer using quartz cells of 10-cm

path lengths. Ultrapure water was used as reference in order to obtain the baseline.

The spectral slope coefficients (S) were inferred from the obtained UV–visible spectra, and for comparison with S values published for rainwater DOM (Kieber et al. 2006; Santos et al. 2009a), S values (μm^{-1}) were calculated from non-linear least-square regressions of the absorption coefficients (a_λ) vs. wavelength for the range between 240 and 400 nm using the equation of Markager and Vincent (2000): $a_\lambda = a_{\lambda o} e^{S(\lambda o - \lambda)} + K$, where λ_0 is the reference wavelength (300 nm) and K is a background parameter to improve the goodness of fit. Absorption coefficients (a_λ, m^{-1}) at each wavelength (λ) were calculated as $a_\lambda = 2.303\, A_\lambda / l$, where A_λ is the corrected spectrophotometer absorbance reading at wavelength λ and l (m) is the optical path length. The maximum wavelength considered for spectral slope calculations was 400 nm since this was the highest wavelength whose absorbance values were consistently above the detection limit.

The molecular fluorescence spectra were obtained using a Fluoromax 3 (JobinYvon-Spex Instruments S.A., Inc., now HORIBA Jobin Yvon Inc., Edison, NJ, USA) with a xenon lamp as the source of radiation. Fluorescence intensity measurements were carried out under thermostated conditions at 20 °C, and spectra were recorded using 1-cm cells and 5-nm bandpasses on both the excitation and the emission monochromators. Excitation–emission matrix (EEM) fluorescence spectra were obtained by concatenating emission spectra measured every 5 nm from 290 to 510 nm using excitation wavelengths (λ_{ex}) from 240 to 400 nm increasing also at 5-nm intervals. Scans were corrected for instrument configuration using factory supplied correction factors (Coble et al. 1993), and data were normalised to a daily-determined water Raman intensity ($275_{ex}/303_{em}$, 5-nm bandpasses) and converted to Raman normalised quinine sulphate (QS) equivalents in ppb (Coble et al. 1998). For each sample, a daily blank (Milli-Q water) spectrum was subtracted from each sample spectrum. Replicate scans within 5 % agreement in terms of intensity and within bandpass resolution in terms of band location were obtained. Due to the low absorbance of rainwater samples, no inner filter effect correction was applied.

Trajectories of air masses and meteorological data

The general characteristics of air masses during the sampling period were evaluated using the Hybrid Single Particle Lagrangian Integrated Trajectory Model (HYSPLIT) developed by Draxler and Rolph (2003) at the National Oceanic Atmospheric Administration—Air Resources Laboratory (NOAA/ARL) (available at www.arl.noaa.gov/HYSPLIT.php). Trajectories were generated for a 48-h hind-cast starting at 10- and 500-m level, calculated every 6 h for every day (24 h) when sampling of precipitation occurred (five trajectories corresponding to 24 h of sampling).

Samples were classified into five groups according to the origin and trajectory of the air masses: class A contains samples related to air masses transported from the Atlantic Ocean; class B represents samples with origins in central and northern parts of industrialised Europe and transported to Portugal over the ocean; class C contains samples with similar origins to those of class B, but transported over land; class D refers to air masses transported from north Africa and the Mediterranean across the Iberian Peninsula; samples in which less than 60 % of the air mass trajectories were from one section only, and had therefore a mixed origin, were agglomerated into class M. A similar classification approach has been previously used by Pio et al. (1991) for rainwater also collected at Aveiro (Portugal). Figure 1a and b shows the air mass trajectory analysis at 10- and 500-m level, respectively, for one of the bulk deposition samples (RS1) collected for this study in order to exemplify the classification of sample according to air mass origins and trajectories.

A meteorological station at the sampling site (at 10-m height) supplied the following information during the sampling period: direction and velocity of wind, relative humidity, air temperature and amount of precipitation.

Results and discussion

Forty bulk deposition samples were collected between September 2008 and September 2009. During this sampling period, approximately 423 mm of rainwater was collected, which represents approximately 50 % of total precipitation (839 mm). Eighty one percent of collected rainwater amount (RA) was related with air masses transported from the Atlantic Ocean (class A) while the rest of precipitation was related to air masses with anthropogenic and terrestrial contributions (3 % of class B and 16 % of class D). A similar distribution was obtained considering all the rainfall events of sampling period instead of only those corresponding to the samples collected. Pio et al. (1991) had also observed that around 80 % of the rainfall in Aveiro between 1986 and 1989 was associated with air masses of Atlantic origin. Regarding the RA by season for collected samples, 13 % occurred in summer (96 % of class A, 1 % of class B and 3 % of class D), 21 % in autumn (80 % of class A, 13 % of class B and 7 % of class D), 35 % in winter (66 % of class A and 34 % of class D) and 31 % in spring (91 % of class A and 9 % of class D).

The volume-weighted average (VWA) DOC concentration and volume-weighted standard deviation for the 40 bulk deposition samples was 0.66±0.09 mg L^{-1}. The range of DOC varied from a low limit of 0.15 mg L^{-1} to a high limit

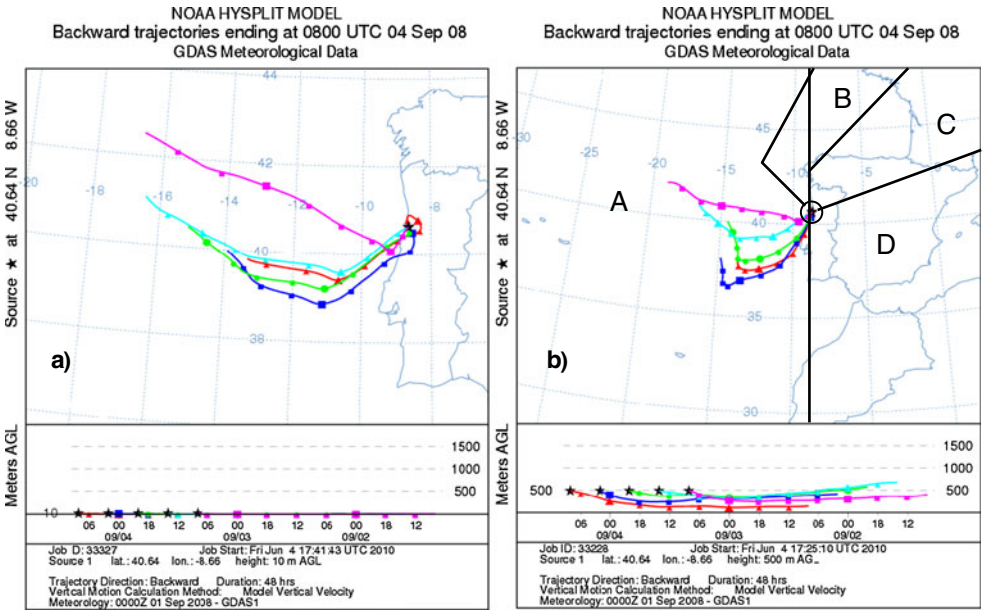

Fig. 1 The air mass trajectory analysis at 10-m (**a**) and 500-m (**b**) level, for the bulk deposition sample (RS1) collected at 4 September 2008, to exemplify the classification of samples according to air-mass origins and trajectories into four groups A, B, C and D

of 6.75 mg L^{-1}. The VWA DOC concentration of collected samples is in the range of those measured at Aveiro in 2005–2006 (0.93±0.87 mg L^{-1}; Santos et al. 2009b).

The VWA absorbance spectra for all bulk deposition events are shown in Fig. 2 along with the VWA spectra for samples of the autumn, winter, spring and summer events (Fig. 2a) and with the VWA spectra for samples of the classes A, B and D (Fig. 2b). The UV–visible spectra of the collected samples are very similar to those obtained for other natural humic substances, decreasing monotonically with increasing wavelength (Senesi et al. 1989), as well as similar to the UV–visible spectra obtained previously for rainwater (Kieber et al. 2006; Mladenov et al. 2009; Santos et al. 2009b). It should be recalled, however, that absorbance at shorter wavelengths (<240 nm) has also a contribution from inorganic species, specifically nitrate, which are likely to be present in rainwater samples (Pio et al. 1991). The VWA absorbance spectra of the samples exhibit a shoulder in the 250–300 nm (~280 nm) region. In aquatic humic substances, absorbance in this UV region is usually attributed to π–π* electronic transitions in phenolic arenes, aniline derivatives, polyenes and polycyclic aromatic hydrocarbons with two or more rings (Chin et al. 1994; Peuravuori and Pihlaja 1997).

Figure 3a presents the EEM fluorescence spectrum of a bulk deposition sample, which may be representative of spectra of all collected samples. Seven bands with different excitation and emission wavelength maxima ($\lambda_{ex}/\lambda_{em}$) can be highlighted: three humic-like bands, A ($\lambda_{ex}/\lambda_{em}$≈240/405 nm), M ($\lambda_{ex}/\lambda_{em}$≈300/410 nm) and C (≈330/420 nm); and four protein-like bands, B_1 ($\lambda_{ex}/\lambda_{em}$≈240/305 nm), B_2 ($\lambda_{ex}/\lambda_{em}$≈270/305 nm), T_1 ($\lambda_{ex}/\lambda_{em}$≈240/340 nm) and T_2 ($\lambda_{ex}/\lambda_{em}$≈275/330 nm). These fluorescence bands that have been found in rainwater (Kieber et al. 2006; Muller et al. 2008; Mladenov et al. 2009; Santos et al. 2009a,b) have also been found in most EEMs of aquatic samples even though the limits for the ranges of their λ_{exc} and λ_{em} maxima can be slightly different from those observed for rainwater samples (Coble 1996; Burdige et al. 2004). Bands A and C have been generally assigned to humic-like compounds, while band M has been usually assigned to marine humic-like compounds. Bands at the same $\lambda_{ex}/\lambda_{em}$ than B_1, B_2 and T_1, T_2 are attributed

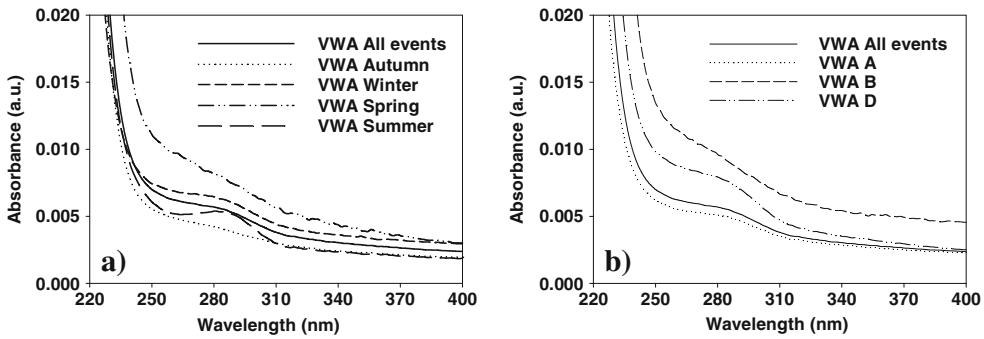

Fig. 2 Volume-weighted average (VWA) UV–visible spectra (absorbance units) versus wavelength (nm) of bulk deposition from: autumn, winter, spring, summer and all events (**a**); classes of trajectories A, B, D and all events (**b**)

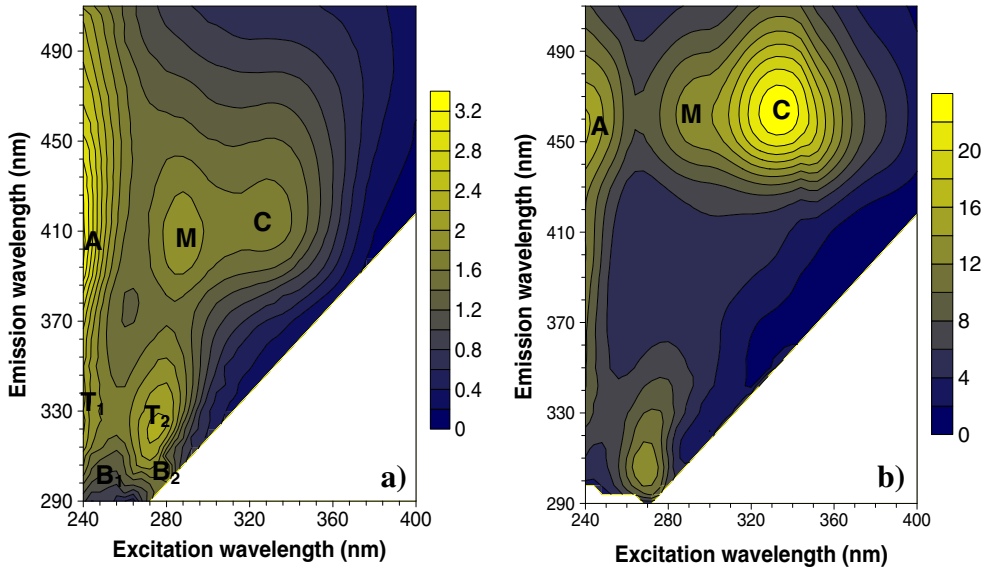

Fig. 3 **a** Representative EEM fluorescence spectrum of bulk deposition CDOM [RS39; collected in summer; associated with maritime air masses; DOC=0.66 mg L^{-1}; UV_{250nm}=0.009 (a.u.); ε_{280nm}=18.6 L g^{-1} C cm^{-1}; spectral slope coefficient=11.5 μm^{-1}; entire scan integrated fluorescence=33.8×10^3; A/M ratio=1.7]. **b** EEM fluorescence spectrum of RS1 bulk deposition sample [collected in summer; associated with maritime air masses; DOC=5.75 mg L^{-1}; UV_{250nm}=0.017 (a.u.); ε_{280nm}=1.8 L g^{-1} C cm^{-1}; spectral slope coefficient=17.8 μm^{-1}; entire scan integrated fluorescence=208.1×10^3; A/M ratio=1.3]. The scale is in ppb QS

to protein-like compounds, such as tyrosine (B_1, B_2) and tryptophan (T_1, T_2). Burdige et al. (2004) used the nomenclature S and R for designating the bands B_1 and T_1, and B and T for designating B_2 and T_2. The humic-like band C does not show up in all the EEM fluorescence spectra of bulk deposition from Aveiro, appearing clearly only in some events (Santos et al. 2009b) and varying its emission wavelength maximum much more than observed for other bands. The variation of emission wavelength of bands may be due to the degree of condensed aromatic rings and other unsaturated bond systems associated (Chen et al. 2002). However, as shown in Fig. 3, fluorescent CDOM is a common component in collected bulk deposition samples.

Figure 4a shows the absorbance at 250 nm (UV_{250nm}) and the entire scan integrated fluorescence for each rain event as functions of DOC. UV_{250nm} was chosen because it may be used as a way of assessing OM content (Duarte and Duarte 2005). The entire scan integrated fluorescence was determined integrating the volume of the three-dimensional surface of EEM fluorescence spectrum. A significant positive correlation between UV_{250nm} (r=0.826, p< 0.001) and integrated fluorescence (r=0.832, p<0.001) with DOC concentration was observed, which may suggest that CDOM is a contributor of DOC in samples. On the other hand, the entire scan integrated fluorescence for each rain event was also plotted against the UV_{250nm} values as shown in Fig. 4b, and a strong positive correlation was found between these two parameters (r=0.819, p<0.001)

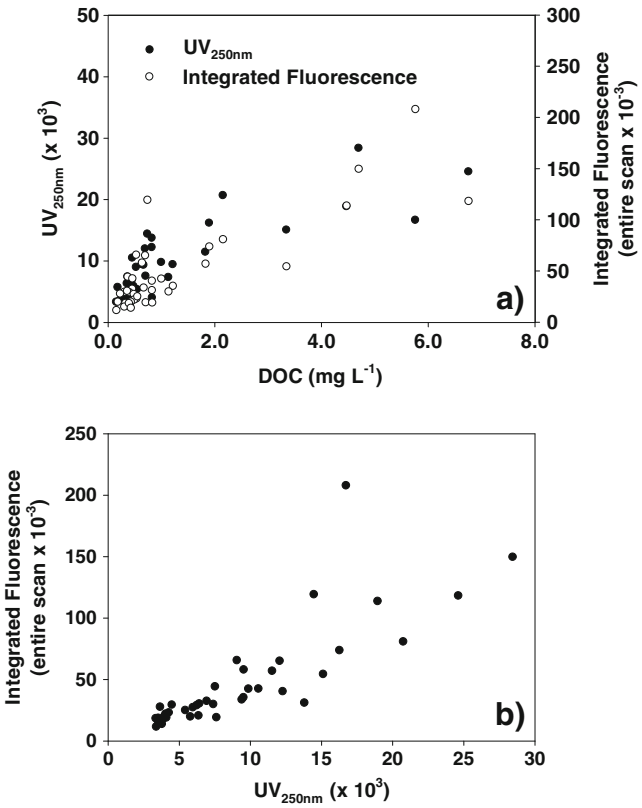

Fig. 4 **a** The relationships between absorbance at 250 nm and DOC (absorbance units; r=0.826, p<0.001), and between entire scan integrated EEM fluorescence and DOC (integrated fluorescence units; r= 0.832, p<0.001). **b** The relationship between the entire scan integrated EEM fluorescence with the absorbance at 250 nm (r=0.819, p<0.001)

suggesting that these optical properties are directly interconnected and that a constant fraction of DOM fluoresces. Kieber et al. (2006) also observed that CDOM was a common component of the DOC pool in rainwater samples of Wilmington (USA), and that a strong correlation occurred between total integrated fluorescence and the absorbance coefficient at 300 nm in rain events. Thus, these findings suggest a similar trend of correlation of the parameters absorbance, entire scan integrated fluorescence and DOC, in bulk deposition and in rainwater.

Figure 5 shows that inverse relationships exist between DOC, UV_{250nm} and integrated fluorescence intensities and the rainwater volume, highlighted by first-order exponential decay curves. These findings suggest that most of CDOM present in samples was washed out from the atmosphere during precipitation events, which was also observed by Kieber et al. (2006) for other rainwater samples collected in Wilmington, Delaware. The sample with the highest value for integrated fluorescence and also with the second highest value of DOC (RS1) also showed some differences in fluorescence properties relatively to the other samples, as will be discussed with data presented in Table 2, and thus, they may be considered outliers. The symbols "x" mark the data corresponding to sample RS1, as shown in Fig. 5, and they were not considered for purpose of curve fitting.

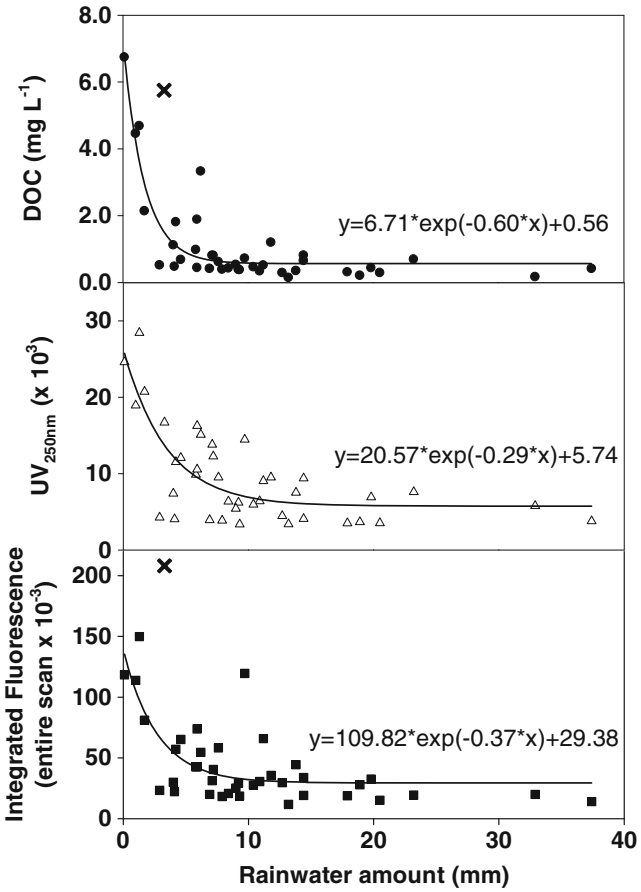

Fig. 5 The variation of DOC concentration (mg L^{-1}; adj. R^2=0.8015, p<0.001), absorbance at 250 nm (absorbance units; adj. R^2=0.570, p< 0.001) and entire scan integrated EEM fluorescence (integrated fluorescence units; adj. R^2=0.493, p<0.001) with rainwater amount (mm). The cross marks (x) indicate the values of DOC and integrated fluorescence obtained to sample RS1 and they may be considered outliers

The VWA of DOC, UV_{250nm}, specific absorptivity at 280 nm (ε_{280nm}), spectral slope coefficient (S), integrated fluorescence and A/M ratio for all samples collected, for the samples collected in 2009, for samples grouped by seasons and for samples grouped by air mass trajectories, are shown in Table 1. The VWA DOC was higher in summer and autumn than in winter and spring. Santos et al (2009b) also observed in bulk deposition of Aveiro that the VWA DOC concentration of autumn rainwater samples was higher than that of winter. Higher VWA for UV_{250nm} and integrated fluorescence were also observed for summer and autumn seasons (Table 1), which suggest that there was more CDOM present in bulk deposition samples during these seasons than in winter and spring. The spectral slope has been shown previously to be inversely related to CDOM molecular weight (MW) (Helms et al. 2008), while the ε_{280nm} parameter has been positively correlated with the MW of aquatic humic substances (Chin et al. 1994). Thus, the results of spectral slope and ε_{280nm} presented in Table 1 suggest that in winter the MW of DOM was higher than in summer and autumn, and in turn higher than in spring. The lower MW observed in spring, summer and autumn events may result from increased DOM photodegradation due to increased solar irradiation during these seasons, relative to winter. In the case of spring samples, the photodegradation may have produced less chromophoric compounds as reflected by lower absorbance (UV_{250nm}) and fluorescence (integrated fluorescence) (Table 1). The A/M ratio was similar for spring, summer and autumn events. These findings suggests that in spring, summer and autumn seasons there was a similar proportion of compounds with a higher degree of conjugation and/or aromaticity (M), and of compounds with lower degree of conjugation and/or aromaticity (A) (Chen et al., 2002). Moreover, the A/M ratio was higher in winter than in the other seasons, signifying higher predominance of A fluorophores relatively to the M fluorophores when compared to the other seasons. On the other hand, Kieber et al. (2007) showed that M fluorophores are more photodegraded than A fluorophores which suggest that in spring, summer and autumn samples the lower A/M ratio are not only due to the photodegradation of A fluorophores, but may be also due to the simultaneous photodegradation and influx of M fluorophores. The results obtained for the class A events in different seasons (Table 1) confirm the occurrence of higher A/M ratio in winter events. Kieber et

Table 1 Bulk deposition VWA DOC concentrations (mg L^{-1}), UV absorbance at 250 nm (UV_{250nm}; absorbance units), specific absorptivity at 280 nm (ε_{280nm}; L g^{-1} C cm^{-1}), spectral slope coefficient (μm^{-1}), integrated fluorescence for the entire scan (integrated fluorescence units) and A/M ratio for the total of samples collected, for the samples of the hydrological year 2009, for samples grouped by seasons and for samples classified according to their air masses trajectories (class)

Sampling period/class	DOC (mg L^{-1})	$UV_{250nm} \times 10^3$	ε_{280nm} (L g^{-1} C cm^{-1})	Spectral slope coefficient (μm^{-1})	Integrated fluorescence $\times 10^{-3}$	A/M ratio
Total (n=40)	0.63 (±0.07)	6.9 (±0.7)	12.3 (±2.5)	9.5 (±1.0)	32.6 (±3.4)	2.2 (±0.3)
2009 (n=35)	0.50 (±0.06)	6.4 (±0.7)	12.7 (±2.7)	9.6 (±1.1)	30.5 (±3.8)	2.2 (±0.3)
Autumn (n=11)	0.82 (±0.20)	9.3 (±0.9)	12.7 (±3.0)	9.6 (±1.5)	40.3 (±5.4)	2.0 (±0.3)
Winter (n=12)	0.38 (±0.05)	6.7 (±1.2)	17.2 (±6.0)	7.6 (±1.1)	36.1 (±7.4)	2.6 (±0.6)
Spring (n=11)	0.60 (±0.12)	4.7 (±1.0)	6.6 (±2.3)	11.7 (±2.2)	20.8 (±3.5)	2.0 (±0.5)
Summer (n=6)	1.10 (±0.33)	8.9 (±3.1)	10.7 (±5.6)	9.0 (±3.0)	40.1 (±11.6)	2.1 (±1.0)
Class A (n=30)	0.53 (±0.07)	6.0 (±0.7)	12.3 (±3.0)	9.1 (±1.1)	27.2 (±2.8)	2.2 (±0.3)
Class B (n=3)	1.49 (±0.77)	13.2 (±6.9)	6.6 (±3.3)	11.2 (±5.4)	58.8 (±31.2)	1.6 (±0.8)
Class D (n=7)	0.96 (±0.23)	9.8 (±1.5)	12.3 (±3.6)	11.0 (±2.1)	54.4 (±12.9)	2.4 (±0.7)
Autumn/class A (n=8)	0.48 (±0.06)	8.1 (±1.0)	14.6 (±3.2)	9.2 (±2.0)	35.9 (±6.5)	2.1 (±0.4)
Winter/class A (n=8)	0.31 (±0.04)	5.6 (±1.5)	18.2 (±9.3)	6.5 (±1.4)	25.6 (±5.8)	2.6 (±0.8)
Spring/class A (n=10)	0.54 (±0.11)	4.2 (±1.0)	6.8 (±2.5)	11.2 (±2.4)	19.4 (±3.6)	2.0 (±0.5)
Summer/class A (n=4)	0.99 (±0.26)	8.3 (±2.5)	10.8 (±4.9)	8.9 (±1.8)	37.1 (±7.6)	2.2 (±0.9)
Spring/summer/autumn class D (n=3)	2.13 (±0.66)	12.6 (±3.5)	4.3 (±2.5)	14.3 (±8.0)	49.4 (±10.2)	1.6 (±0.8)
Winter class D (n=4)	0.51 (±0.09)	8.7 (±1.6)	15.4 (±1.8)	9.7 (±0.7)	56.3 (±14.7)	2.8 (±0.5)

The volume-weighted standard deviations are indicated between brackets

n=number of rain events

al. (2006) also found, in rainwater samples from Wilmington, a shift to lower MW CDOM and lower A/M ratio in the summer months.

Table 1 also shows some differences in CDOM for the samples grouped according to classes of air mass trajectories. Bulk deposition samples related to air masses with a maritime origin (class A) showed lower VWA values of DOC, UV_{250nm} and integrated fluorescence, suggesting lower CDOM content than samples with a terrestrial contribution (classes B and D). Samples from class A are associated with air masses transported directly from the Atlantic Ocean, and the VWA values found should approximately represent background concentrations. On the other hand, when air masses come from continental Europe and transported over the ocean (class B), VWA of DOC, UV_{250nm} and integrated fluorescence present the highest values, suggesting that anthropogenic sources are important contributors of CDOM and that this CDOM is efficiently transported long from the sources over the sea. Bulk deposition related to air masses from Mediterranean area (class D) had the intermediate VWA values of DOC, UV_{250nm} and integrated fluorescence, suggesting smaller terrestrial/pollutant input when compared with the air masses from continental Europe, transported over the ocean (class B). Kieber et al. (2006) and Muller et al. (2008) observed that air mass back-trajectory analysis indicated elevated CDOM levels in continentally influenced rainwater relative to marine dominated events implying that anthropogenic and/or terrestrial sources are also important contributors to CDOM in precipitation. Spectral slope and the ε_{280nm} also suggest that bulk deposition DOM from continental Europe and transported over the ocean (class B) have lower MW than bulk deposition DOM from the ocean (class A) and from the Mediterranean area (class D). As samples of class B were all collected in summer and autumn, the lower MW of DOM may be due to the photodegradation that occurred with the higher irradiance during these seasons, as suggested above. Moreover, separating the events of the class D in spring/summer/autumn and winter events (Table 1), it was also observed lower MW DOM for samples from seasons with higher irradiance. On the other hand, the A/M ratio is lower for DOM from samples of class B and of class D in spring/summer/autumn than for DOM of class A, indicating higher relative predominance of organic compounds with higher degree of conjugation or aromaticity, which may be due to the origin of air mass trajectory and respective anthropogenic/terrestrial sources.

Comparing the results obtained for the bulk deposition of Aveiro with that of Kieber et al. (2006) for the rainwater of Wilmington, besides similar DOC content for the total of samples at both sites, the DOM of bulk deposition of Aveiro had higher MW (>ε_{280nm} and <spectral slope coefficient) and higher predominance of fluorophores with lower degree of conjugation and aromaticity (>A/M). In

a recent study, Santos et al. (2009a) concluded that the DOM in Aveiro bulk deposition during autumn consists of a complex mixture of hydroxylated and carboxylic acids with a predominantly aliphatic character, containing a minor component of aromatic structures. The authors also suggested that the oxidation of volatile organic compounds directly emitted into the atmosphere, either by anthropogenic or biogenic sources, may be an important contribution to the polyacidic nature of bulk deposition DOM through in-cloud and/or precipitation scavenging of aerosol particles.

Table 2 shows the average excitation and emission wavelength maxima of the fluorescence of the humic-like bands (A, M, C) and their VWA of fluorescence intensity (FI) and of specific fluorescence intensity (SFI) for samples grouped by seasons and for samples grouped by air masses trajectories (class). As shown in Table 2, the average values of excitation/emission wavelengths maxima for each of the humic-like bands (A, M and C) were similar for all the samples: A ($\lambda_{ex}/\lambda_{em}\approx$ 240/405 nm), M ($\lambda_{ex}/\lambda_{em}\approx$300/410 nm) and C ($\lambda_{ex}/\lambda_{em}\approx$330/420) nm. On other hand, while the ranges of excitation wavelengths were small for all bands, the ranges of emission wavelengths maxima were large in summer for bands A and M when air mass trajectories were maritime (class A) and large for band C in all seasons and in all classes of air mass trajectories. A more detailed analysis of the samples showed that only one summer sample [RS1, associated with maritime air mass (class A)] was responsible for increasing the emission wavelength range of humic-like bands (Fig. 3b): 415 to 455 nm in band A, 425 to 455 nm in band M and 445 to 460 nm in band C. That sample is presented in Fig. 1 and as it may be seen, the trajectories of air mass at a 10-m height highlight the passage for the city of Coimbra (at south of Aveiro) and for the industrialised area at north of Aveiro (town of Estarreja). Thus, this bulk deposition sample may have been affected by anthropogenic sources and consequently humic-like bands were shifted to longer emission wavelengths comparatively to the other samples, indicating the presence of more condensed aromatic rings and other unsaturated bond systems (Chen et al. 2002). Although without this sample (RS1) the ranges of emission wavelengths decrease for bands A and M in summer, being small, for band C the ranges continue to be large, which may be due to its large uncertainty resulting from the less precise definition in some samples. Nevertheless, no clear relationship was found between locations of emission wavelengths maxima of band C of samples with the seasons and air mass trajectories.

The VWA FI of bands A, M and C is lower for spring than for the other seasons (Table 2), indicating a low content of fluorescent organic matter in spring. This fact is not attributable to a lower DOM concentration because, as seen in Table 1, the DOC concentration in spring is higher than in winter. However, VWA SFI shows that for the same concentration of DOC, the winter season presents the highest fluorescence for the three bands and about double the intensity of spring. Moreover, the SFI of the three bands are lower and closer for spring and summer, and higher and closer for autumn and winter, except for the band A where the SFI for autumn is much less intense than winter. These facts may be due to the occurrence of more photodegradation of all bands in spring and summer relative to autumn and winter, as well as of band A for autumn relative to winter but to a lesser extent, which is in accordance with the lower MW and lower A/M ratio observed for spring, summer and autumn and presented in Table 1.

In addition, Table 2 shows that bulk deposition related with air masses of maritime origin (class A) have lower VWA FI of the fluorescent bands, A, M and C, than rainwater from Mediterranean area (class D) and than rainwater related to air masses from continental Europe and transported over the ocean (class B). This fact supports the idea that samples associated with air masses transported directly from the Atlantic Ocean (class A) may represent background VWA FI values, as mentioned above. Muller et al. (2008) observed that the highest humic-like substance (HULIS) fluorescence intensities in rainwater were associated with events of continental origin and also suggested the influence of terrestrial/anthropogenic sources. On the other hand, the SFI values obtained for all seasons of class A highlight that local sources may have contributed to the fluorescent DOM found in bulk deposition samples, as suggested by the inverse correlations of DOC, UV_{250nm} and integrated fluorescence with rainwater amount (Fig. 5). The value of SFI of band A associated to samples of class B (that occurred in summer and autumn seasons) is higher but more similar to the SFI of spring/summer/autumn samples of class D, suggesting some similar fluorophores, which may be associated with a terrestrial/anthropogenic origin. On other hand, for the bands M and C, the SFI values indicate that fluorophores fluoresce more when bulk deposition is from continental Europe and transported over the ocean (class B) than when bulk deposition from the Mediterranean area (class D) for the seasons spring, summer and autumn, highlighting the slightly more fluorescent organic matter present. These findings suggest that fluorescent compounds that produce bands A, M and C were efficiently transported far from their sources (industrialised Europe), over the sea (class B) and that terrestrial/anthropogenic sources are important contributors to them. In addition, results highlight that bulk deposition

Table 2 Average excitation and emission wavelength maxima (±standard deviation) of the fluorescence of humic-like bands and its VWA of fluorescence intensity (FI; ppb QS) and specific fluorescence intensity (SFI; g^{-1} C L ppb QS) for samples collected at the different seasons and for samples grouped by air masses trajectories (class)

Band	Sampling period/Class	λ_{ex} max (nm)	λ_{em} max (nm)	FI (ppb QS)	SFI (g^{-1} C L ppb QS)	Attribution
A	Autumn (n=11)	240±0	405±6 (395–410)	4.4 (±0.6)	8,322 (±2,334)	Humic-like
	Winter (n=12)	240±0	399±7 (390–415)	4.4 (±0.9)	12,062 (±3,158)	
	Spring (n=11)	240±0	408±8 (395–420)	2.5 (±0.4)	4,853 (±1,326)	
	Summer (n=6)	240±0	405±11 (390–455)	4.3 (±1.0)	3,937 (±1,587)	
	Class A (n=30)	240±0	406±12 (395–455)	3.1 (±0.3)	7,668 (±1,618)	
	Class B (n=3)	240±0	407±3 (405–410)	6.6 (±3.4)	4,475 (±2.221)	
	Class D (n=7)	240±0	400±8 (390–410)	6.6 (±1.5)	10,241 (±3,184)	
	Autumn/class A (n=8)	240±0	404±6 (395–410)	3.9 (±0.7)	9,548 (±2,642)	
	Winter/class A (n=8)	240±0	401±7 (395–415)	3.1 (±0.8)	11,569 (±4,808)	
	Spring/class A (n=10)	240±0	408±8 (395–420)	2.3 (±0.4)	4,968 (±1,458)	
	Summer/class A (n=4)	240±0	419±22 (400–455)	3.6 (±0.5)	3,964 (±1,162)	
	Spring/summer/autumn/class D (n=3)	240±0	408±2 (405–410)	5.7 (±1.5)	3,056 (±1,886)	
	Winter/class D (n=4)	240±0	394±2 (390–395)	6.9 (±1.4)	13,020 (±1,760)	
M	Autumn (n=11)	294±5 (290–305)	410±0	2.4 (±0.3)	4,167 (±1,079)	Marine humic-like
	Winter (n=12)	299±4 (295–305)	409±9 (395–425)	1.7 (±0.3)	4,533 (±1,145)	
	Spring (n=11)	299±2 (295–300)	412±3 (410–415)	1.3 (±0.3)	2,419 (±683)	
	Summer (n=6)	296±5 (285–305)	412±9 (395–455)	2.7 (±0.7)	1,969 (±794)	
	Class A (n=30)	297±5 (285–305)	414±10 (395–455)	1.6 (±0.2)	3,404 (±627)	
	Class B (n=3)	292±3 (290–295)	410±0	4.1 (±2.2)	2,740 (±1,357)	
	Class D (n=7)	295±6 (285–300)	406±4 (400–410)	2.9 (±0.5)	3,937 (±1,096)	
	Autumn/class A (n=8)	295±6 (290–305)	410±0	1.9 (±0.3)	4,655 (±1,240)	
	Winter/class A (n=8)	299±5 (290–305)	413±9 (395–425)	1.2 (±0.3)	4,437 (±1,742)	
	Spring/class A (n=10)	299±2 (295–300)	412±3 (410–415)	1.2 (±0.3)	2,441 (±754)	
	Summer/class A (n=4)	291±5 (285–300)	425±18 (410–455)	2.1 (±0.6)	1,972 (±592)	
	Spring/summer/autumn/class D (n=3)	292±6 (285–300)	410±0	3.7 (±1.0)	1,919 (±1,092)	
	Winter/class D (n=4)	298±3 (295–300)	401±4 (395–405)	2.5 (±0.6)	4,717 (±705)	
C	Autumn (n=11)	328±6 (320–340)	420±13 (405–445)	2.0 (±0.3)	3,677 (±972)	Humic-like
	Winter (n=12)	330±0	418±14 (395–445)	1.4 (±0.3)	3,826 (±920)	
	Spring (n=11)	331±2 (330–325)	424±10 (415–445)	0.9 (±0.2)	1,641 (±440)	
	Summer (n=6)	330±4 (320–340)	422±13 (395–460)	3.6 (±1.3)	1,778 (±655)	
	Class A (n=30)	330±3 (320–340)	423±13 (405–460)	1.4 (±0.2)	2,779 (±508)	
	Class B (n=3)	325±5 (320–330)	428±15 (415–445)	3.6 (±2.0)	2,360 (±1,175)	
	Class D (n=7)	331±2 (330–335)	414±12 (395–435)	2.3 (±0.4)	3,296 (±935)	
	Autumn/class A (n=8)	326±9 (305–335)	417±11 (405–445)	1.7 (±0.3)	4,137 (±1,111)	
	Winter/class A (n=8)	323±11 (305–330)	421±13 (405–445)	1.0 (±0.2)	3,715 (±1,402)	
	Spring/class A (n=10)	332±3 (330–340)	425±9 (415–445)	0.8 (±0.2)	1,658 (±489)	
	Summer/class A (n=4)	330±4 (325–335)	433±18 (415–460)	2.5 (±1.3)	1,770 (±445)	
	Spring/summer/autumn/class D (n=3)	332±2 (330–335)	422±9 (415–435)	2.8 (±0.4)	1,365 (±681)	
	Winter/class D (n=4)	324±6 (315–330)	410±9 (395–420)	2.2 (±0.5)	4,042 (±518)	

The volume-weighted standard deviations of FI and SFI are indicated between brackets. The values in brackets for the excitation and emission wavelengths are the observed ranges for data sets

n=number of rain events

samples associated with terrestrial air masses (classes B and D) presented higher CDOM content than samples with marine air masses (class A), which may be due to the contribution of terrestrial/anthropogenic sources.

Conclusions

The DOM of bulk deposition at a coastal town in south-western Europe (Aveiro) was characterised using UV–visible absorbance and molecular fluorescence spectroscopies and by its DOC content. The seasonal and air mass effects on DOM of bulk deposition were evaluated. The results led to the following conclusions:

1. CDOM is an important contributor to DOC in bulk deposition samples, where compounds with relatively low degrees of conjugation and aromaticity predominate.
2. Bulk deposition samples from summer and autumn presented higher CDOM content and more compounds with higher degrees of conjugation and aromaticity (>FI of bands M and C) than samples from winter and spring. Furthermore, bulk deposition samples from spring, summer and autumn presented lower MW than samples from winter, which may be due to greater DOM photodegradation.
3. Bulk deposition samples related to air masses with a maritime origin (class A) contained less CDOM than samples with terrestrial/anthropogenic contributions. Moreover, bulk deposition samples associated with air masses that come from continental Europe and transported over the ocean (class B) presented higher CDOM content and more organic compounds with higher degrees of conjugation or aromaticity than samples from the Mediterranean area (class D), indicating that anthropogenic sources are important contributors of CDOM and that CDOM was efficiently transported far from sources (industrialised Europe) over the sea (class B).

Chromophoric compounds are shown to be important constituents of DOM of bulk deposition and the presence of these highly absorbing and fluorescing compounds may exert a significant effect on atmospheric absorption of solar radiation. The presence of chromophoric compounds in DOM of bulk deposition is expected to affect terrestrial and aquatic ecosystems, as rainwater is the predominant source of fresh water, and may have important implications for human health.

Acknowledgments Authors acknowledge funding from the Portuguese FCT (Foundation for Science and Technology) to CESAM (Centre for Environmental and Marine Studies). The FCT fellowship given to P.S.M. Santos (Ref. SFRH/BPD/75350/2010) is also acknowledged. Authors would like to gratefully thank the Group of Organic Chemistry of University of Aveiro for making available to us the use of their Fluoromax 3 equipment of molecular fluorescence spectrophotometer. TOC analyses were carried out at the "Administração Regional de Saúde" (Aveiro) and authors wish to here express their gratitude to this Centre and especially to Dra. Ana Maria Félix and Dra. Rosário Figueiredo. The authors also wish to thank Professor Maria Dolores Orgaz from the Department of Physics at the University of Aveiro for meteorological information support.

References

Andreae MO, Jones CD, Cox PM (2005) Strong present-day aerosol cooling implies a hot future. Nature 435:1187–1190

Burdige DJ, Kline SW, Chen W (2004) Fluorescent dissolved organic matter in marine sediment pore waters. Mar Chem 89:289–311

Chen J, Gu B, LeBoeuf EJ, Pan H, Dai S (2002) Spectroscopic characterization of the structural and functional properties of natural organic matter fractions. Chemosphere 48:59–68

Cheng Y-y, Guo W-d, Long A-m, Chen S-y (2010) Study on optical characteristics of chromophoric dissolved organic matter (CDOM) in rainwater by fluorescence excitation–emission matrix and absorbance spectroscopy. Spectrosc Spect Anal 30:2413–2416

Chin Y-P, Alken G, O'Loughlin E (1994) Molecular weight, polydispersity, and spectroscopic properties of aquatic humic substances. Environ Sci Technol 28:1853–1858

Coble PG, Schultz CA, Mopper K (1993) Fluorescence contouring analysis of DOC Intercalibration Experiment samples: a comparison of techniques. Mar Chem 41:173–178

Coble PG (1996) Characterization of marine and terrestrial DOM in seawater using excitation emission matrix spectroscopy. Mar Chem 51:325–346

Coble PG, Del Castillo CE, Avril B (1998) Distribution and optical properties of CDOM in the Arabian Sea during the 1995 Southwest Monsoon. Deep-Sea Res II 45:2195–2223

Decesari S, Facchini MC, Fuzzi S, Tagliavini E (2000) Characterization of water-soluble organic compounds in atmospheric aerosols: a new approach. J Geophys Res 105:1481–1489

Draxler RR, Rolph GD (2003) HYSPLIT (Hybrid Single-Particle Lagrangian Integrated Trajectory), www.arl.noaa.gov/HYSPLIT.php. NOAA Air Resources Laboratory, Silver Spring

Duarte RMBO, Duarte AC (2005) Application of non-ionic solid sorbents (XAD resins) for the isolation and fractionation of water-soluble organic compounds from atmospheric aerosols. J Atmos Chem 51:79–93

Duarte RMBO, Pio CA, Duarte AC (2005) Spectroscopic study of the water-soluble organic matter isolated from atmospheric aerosols collected under different atmospheric conditions. Anal Chim Acta 530:7–14

Facchini MC, Fuzzi S, Zappoli S, Andracchio A, Gelencsér A, Kiss G, Krivácsy Z, Mészáros E, Hansson HC, Alsberg T, Zebühr Y (1999) Partitioning of the organic aerosol component between fog droplets and interstitial air. J Geophys Res 104(26):26821–26832

Gysel M, Weingartner E, Nyeki S, Paulsen D, Baltensperger U, Galambos I, Kiss G (2004) Hygroscopic properties of water-soluble matter and humic-like organics in atmospheric fine aerosol. Atmos Chem Phys 4:35–50

Helms JR, Stubbins A, Ritchie JD, Minor EC, Kieber DJ, Mopper K (2008) Absorption spectral slopes and slope ratios as indicators of molecular weight, source, and photobleaching of chromophoric dissolved organic matter. Limnol Oceanogr 53:955–969

Hoffer A, Kiss G, Blazsó M, Gelencsér A (2004) Chemical characterization of humic-like substances (HULIS) formed from a lignin-type precursor in model cloud water. Geophys Res Lett 31: L06115. doi:10.1029/2003GL018962

Kieber RJ, Whitehead RF, Reid SN, Willey JD, Seaton PJ (2006) Chromophoric dissolved organic matter (CDOM) in rainwater, Southeastern North Carolina, USA. J Atmos Chem 54:21–41

Kieber RJ, Willey JD, Whitehead RF, Reid SN (2007) Photobleaching of chromophoric dissolved organic matter (CDOM) in rainwater. J Atmos Chem 58:219–235

Markager S, Vincent WF (2000) Spectral light attenuation and the absorption of UV and blue light in natural waters. Limnol Oceanogr 45:642–650

Mladenov N, López-Ramos J, McKnight DM, Reche I (2009) Alpine lake optical properties as sentinels of dust deposition and global change. Limnol Oceanogr 54:2386–2400

Miller C, Gordon KG, Kieber RJ, Willey JD, Seaton PJ (2009) Chemical characteristics of chromophoric dissolved organic matter in rainwater. Atmos Environ 43:2497–2502

Muller CL, Baker A, Hutchinson R, Fairchild IJ, Kidd C (2008) Analysis of rainwater dissolved organic carbon compounds using fluorescence spectroscopy. Atmos Environ 42:8036–8045

Peuravuori J, Pihlaja K (1997) Molecular size distribution and spectroscopic properties of aquatic humic substances. Anal Chim Acta 137:133–149

Pio CA, Salgueiro ML, Nunes TN (1991) Seasonal and air-mass trajectory effects on rainwater quality at the South-Western European border. Atmos Env 25A:2259–2266

Santos PSM, Otero M, Duarte RMBO, Duarte AC (2009a) Spectroscopic characterization of dissolved organic matter isolated from rainwater. Chemosphere 74:1053–101

Santos PSM, Duarte RMBO, Duarte AC (2009b) Absorption and fluorescence properties of rainwater during the cold season at a town in Western Portugal. J Atmos Chem 62:45–57

Santos PSM, Otero M, Santos EBH, Duarte AC (2010) Molecular fluorescence analysis of rainwater: effects of sample preservation. Talanta 82:1616–1621

Seitzinger SP, Styles RM, Lauck R, Mazurek MA (2003) Atmospheric pressure mass spectrometry: a new analytical chemical characterization method for dissolved organic matter in rainwater. Environ Sci Technol 37:131–137

Senesi N, Miano TM, Provenzano MR, Brunetti G (1989) Spectroscopic and compositional comparative characterization of I.H.S.S. reference and standard fulvic and humic acids of various origins. Sci Total Environ 81:143–156

Willey JD, Kieber RJ, Eyman MS, Avery GB (2000) Rainwater dissolved organic carbon: concentrations and global flux. Global Biogeochem Cy 14:139–148

Zappoli S, Andracchio A, Fuzzi S, Facchini MC, Gelencsér A, Kiss G, Krivácsy Z, Molnár Á, Mészáros E, Hansson HC, Rosman K, Zebühr Y (1999) Inorganic, organic and macromolecular components of fine aerosol in different areas of Europe in relation to their water solubility. Atmos Environ 33:2733–2743